Shelling, J. G., Bjornson, M. E., Hodges, R. S., Taneja, A. K., & Sykes, B. D. (1984) *J. Magn. Reson. 57*, 99–114.
Szebenyi, D. M. E., Obendorf, S. K., & Moffatt, K. (1981) *Nature (London) 294*, 327–332.
Vogel, H. J., Drakenberg, T., Forsén, S., O'Neil, J. D. J., & Hofmann, T. (1985) *Biochemistry* (submitted for publication).
Wallace, R. W., Tallant, E. A., Dockter, M. E., & Cheung, W. Y. (1982) *J. Biol. Chem. 257*, 1845–1854.
Wasserman, R. H. (1980) in *Calcium-Binding Proteins: Structure and Function* (Siegel, F. L., Carafoli, E., Kretsinger, R. H., MacLennan, D. H., & Wasserman, R. H., Eds.) pp 357–361, Elsevier North-Holland, New York.
Wasserman, R. H., Fullmer, C. S., & Taylor, A. N. (1978) in *Vitamin D* (Lawson, D. E. M., Ed.) pp 133–166, Academic Press, New York.
Williams, T. C., Corson, D. C., & Sykes, B. D. (1984) *J. Am. Chem. Soc. 106*, 5698–5702.

500-MHz Proton NMR Studies of the Medium-Dependent Conformational Preference of Prostaglandin $F_2\alpha$ Analogues†

Niels H. Andersen* and Bor-Sheng Lin
Chemistry Department, University of Washington, Seattle, Washington 98195
Received May 3, 1984; Revised Manuscript Received September 18, 1984

ABSTRACT: The complete assignments of the ^1H NMR spectra of 2–10 mM D_2O solutions of prostaglandin $F_2\alpha$ ($PGF_2\alpha$), its C-15 epimer, and analogues bearing a *gem*-dimethyl group at C-16 or C-17 are presented. $PGF_2\alpha$ and its 1,9- and 1,15-lactones were similarly studied in $CDCl_3$ solution. The assignments follow from extensive scalar decoupling and difference NOE spectra and the examination of a specifically deuterated analogue. These studies also define the conformation (including cyclopentane pseudorotational preference) from C-5 through C-16 in each system. The macrolides show little or no conformational freedom at C-4 → C-1, but extensive rotational averaging occurs in the terminal portions of both side chains in the monocyclic compounds. The conformational features so determined are contrasted to those seen in crystal structures and those postulated to occur upon binding to $PGF_2\alpha$-recognizing receptors. The NMR data run counter to the DeTitta hypothesis that changes in the orientation of the C-13,14 π-bond nodal plane relative to the cyclopentane ring and the C-15–O bond are recognition determinants at $PGF_2\alpha$-specific receptors and account for the medium-dependent chiroptical spectral changes previously reported.

The prostaglandins (PGs),[1] a branch of the arachidonate cascade, are ubiquitous in human tissues and display diverse and often opposing physiologic effects even though they all are remarkably similar in structure. At least 13 distinct classes of PG receptors must be postulated[2] on the basis of pharmacologic and structure–activity relationship studies. Most of the receptors show remarkable selectivity in their ability to recognize specific PGs with minimal cross-reactivity with other types of prostaglandins. A detailed understanding of the conformational preferences of the different classes of prostaglandins appears to be essential as a basis for ascertaining the stereostructural requisites for these biorecognition phenomena.

To date, X-ray crystallography (DeTitta et al., 1980, and references cited therein), CD spectroscopy (Leovey & Andersen, 1975a; Andersen et al., 1976), and NMR have been the tools applied in the study of PG structures. The very first PG crystal structure, of a $PGF_1\beta$ derivative (Abrahamsson, 1963), revealed close proximity and specific alignment of the two side chains. Such "aligned side-chain" or "hairpin" models (Rabinovitch et al., 1971; Andersen & Ramwell, 1974) have been the basis of much of the SAR analysis of PGs to date. Three "hairpinlike" $PGF_2\alpha$ structures observed in the solid state are shown in Figure 1. However, PG structures are a priori highly flexible arrays, and computer conformational modeling confirms this. For example, Murakami & Akahori (1977) noted that their analysis yielded 210 conformers of PGE_1 falling within 3 kcal/mol of the most stable one. This conformational versatility results from the pseudorotational possibilities of the cyclopentane ring (Figure 2) combined with rotameric equilibria in the unrestrained side chains. Nonetheless, X-ray crystallographers have, in the discussion of PG biorecognition mechanisms, stated "...with confidence that the crystallographically observed conformations of prostaglandins are the biologically relevant ones at the receptor site" (Langs et al., 1977). If PGs are as flexible as suggested by molecular dynamic calculations, neither solid phase nor free solution conformations are a trustworthy guide to the receptor-bound states. Elucidation of the conformation of PG in dilute aqueous media is, however, directly pertinent to the receptor recognition phenomenon. Changes in aqueous media conformational preference of analogue structures will, of necessity, be related to potency. For a series of analogues which all bear the requisite pharmacophore moieties and which can attain the conformation required at the receptor without violating the

† This work was supported by NIH Research Grants GM-20848 and HL-23103. Contracts N01-HD-4-2839 and HD-8-2808 provided support for the synthesis of some of the analogues examined.

[1] Abbreviations: PG, prostaglandin; CD, circular dichroism; NMR, nuclear magnetic resonance; NOE, nuclear Overhauser effect; DSS, 4,4-dimethyl-4-silapentane-1-sulfonate; FID, free induction decay; SAR, structure–activity relationship; SPT, selective population transfer; NOESY, NOE spectroscopy via the 2D cross-relaxation experiment; 2D, two dimensional; EDTA, ethylenediaminetetraacetic acid; GC/MS, gas chromatography/mass spectroscopy; S/N, signal to noise; FT, Fourier transform.

[2] Prostanoid SAR's that have led to this conclusion and a classification of the receptors by action mediated and type of PG recognized can be found in Andersen (1985).

0006-2960/85/0424-2338$01.50/0

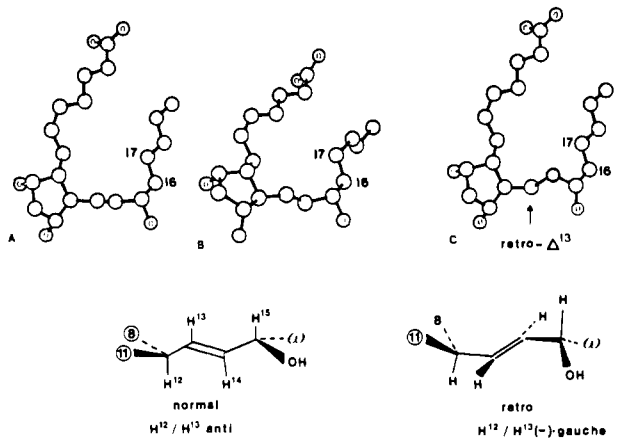

FIGURE 1: Projection of the solid-state structures of $PGF_2\alpha$ (A–C) normal to the C12–C15–O15 plane. The views are taken from a handout entitled "Molecular Conformations of the Prostaglandins: A Review of the Crystallographic Results" by G. T. DeTitta. The details of conformation about the trans Δ^{13} unit are shown. The boldly numbered carbons show the Me_2 substitution positions in the analogues examined.

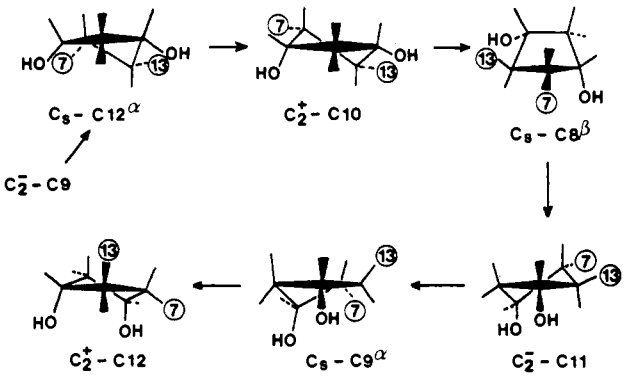

FIGURE 2: Partial pseudorotational itinerary (illustrated by a $PGF_2\alpha$ structure fragment) which includes all of the cyclopentane conformers observed in PG crystal structures (DeTitta et al., 1980).

steric constraints of the receptor pocket, the extent (in kcal/mol) to which the preferred aqueous geometry lies at lower energy than the receptor conformation will be reflected in a reduced receptor affinity. An analogue with an altered conformational equilibrium presents a lower effective concentration of the recognized pharmacophore. High-resolution pulsed NMR is potentially the most informative spectroscopic tool for studying both molecular structure and dynamics in solution. Kotovych and co-workers (1980a,b, 1982) have studied a variety of prostaglandins at 400 MHz, but these studies have typically been in organic solvents or at unrealistically high concentrations. $PGF_2\alpha$ (and its analogues), which have played a key role in the evolution of the hairpin conformation pharmacophore model, have not been the subject of a detailed structural investigation by modern NMR methods. The previous study, due to Conover & Fried (1974), which was carried out at 270 MHz, failed to assign all of the resonances and reversed the assignment of key protons on the cyclopentane ring. We report herein the full spectral assignments for $PGF_2\alpha$ and some of its analogues which will serve as the base-line study for subsequent motional and receptor binding investigations.

Materials and Methods

Prostaglandins. $PGF_2\alpha$, 15-*epi*-$PGF_2\alpha$, 16,16-dimethyl-$PGF_2\alpha$, 17,17-dimethyl-$PGF_2\alpha$, $PGF_2\alpha$-1,9-olide, and $PGF_2\alpha$-1,15-olide were available from previous synthetic efforts (Andersen et al., 1977, 1981a,b). With the exception of $PGF_2\alpha$, the samples were greater than 97% enantiomeric excess of the natural form by CD assay. $PGF_2\alpha$ was the crystalline racemate form, mp 62–63 °C (Andersen & Leovey, 1974). Comparison spectra of $PGF_2\alpha$ methyl ester employed the natural form obtained by CH_2N_2/Et_2O treatment of synthetic (+)-$PGF_2\alpha$. $PGF_2\alpha$-*3,3,4,4-d*$_4$ was purchased from Merck Sharp & Dohme (Canada) and assayed 92% d_4, 5.8% d_3, ≲1% d_2, and ≲2% d_0 by GC/MS on the methyl ester tris(trimethylsilyl) derivative.

Sample Preparation. Solutions of 2–20 mM $PGF_2\alpha$ and its analogues in buffered D_2O (99.96%) or $CDCl_3$ (99.8%) were degassed thoroughly by the freeze–pump–thaw procedure several times and sealed under argon in 5-mm NMR tubes. The phosphate-buffered D_2O solutions were prepared from K_2HPO_4, KH_2PO_4, and 99.8% D_2O to nominal pH (glass electrode) without correction for D_2O activity and then lyophilized and reconstituted to volume in 99.96% D_2O.

NMR Spectra. All spectra were obtained at 293 K (unless otherwise indicated) on a Bruker WM-500 pulsed FT NMR spectrometer employing an Aspect 2000 computer for signal accumulation and Fourier transformation. Standard parameters for normal spectra were 4000-Hz spectral width, 10-μs pulse length, 32K channel quadrature detection (0.24 Hz/real point), and 5-s preparatory relaxation delay. FIDs were accumulated until a sufficient S/N was obtained, transformed, and recorded at ca. 2 mm/Hz. Chemical shifts are reported (±0.5 Hz) in parts per million from DSS (D_2O spectra) or tetramethylsilane ($CDCl_3$ spectra). Key line frequencies were read off of the oscilloscope display via the cursor. Coupling constants were obtained by first-order analysis. In most cases splittings were read directly as separations of interpolated peak positions (±0.05 Hz) observed on oscilloscope displays of resolution-enhanced 32K real point spectra. Resolution enhancement was achieved by Gaussian multiplication corresponding to a line-broadening value of LB = −0.5 Hz. Prior to resolution enhancement individual lines of well-defined multiplets displayed widths at half-height of ca. 1.4 (in D_2O) or 1.0 Hz (in $CDCl_3$).

Resonance assignments came from extensive series of homonuclear spin–spin decoupling and NOE experiments. The spin decoupling experiments were performed by applying a continuously effective saturating power (15–25 mW) to the desired resonance while accumulating the FIDs. Difference nuclear Overhauser enhancement (ΔNOE) spectra were obtained by Fourier transformation of the difference FIDs accumulated by the following protocol.[3] The decoupler, operating in the gated mode, was set on-resonance for a time about 5 times the T_1 value of the proton to build up the NOE. It was gated off during acquisition. Eight FID signals were accumulated. The memory was then negated, and the experiment was repeated with the decoupler off-resonance. The cycle was repeated until the required number of transients was accumulated. Percent NOEs were calculated from the integrated difference spectrum by using the integral of the irradiated resonance as the −100% standard. Spectra simplification was achieved in some shift regions by the inversion–recovery method, using a PD–180°–τ–90°–AQ pulse sequence. The preparatory relaxation delay time (PD) was 5 times the longest T_1 observed.

Studies of Pr(III)-induced shifts were performed as follows. A deoxygenated buffered (20 mM PO_4) D_2O solution of prostaglandin (5 mM), EDTA (8 mM), $La(NO_3)_3$ (5 mM), and DSS (1 mM as chemical shift standard) was prepared,

[3] The protocol corresponds to the block-difference accumulation method of Chapman et al. (1978).

Table I: Concentration and Solvent Dependence of Selected $PGF_2\alpha$ NMR Chemical Shifts[a]

	$PGF_2\alpha$ Me ester	$PGF_2\alpha$ free acid form					
		$CDCl_3$ at		D_2O solutions at			
	$CDCl_3$	20 mM	5 mM	600 mM[b]	20 mM[b]	10 mM	2 mM
H-2	δ2.322	δ2.338	2.342	δ2.25	2.22	2.212	2.198
H-4a,b	2.11, 2.09	2.138[c]	2.14, 2.12	2.17	2.14	2.085[c]	2.086[c]
H-6	5.43	5.468	5.485	5.35	5.54	5.555	5.560
H-7a,b	2.28, 2.10	2.20, 2.17	2.17[c]	2.06	2.09	2.168[c]	2.19[c]
H-9	4.158	4.172	4.195	4.16	4.23	4.228	4.230
H-10a	2.203	2.233	2.22	2.46	2.52	2.516	2.520
H-10b	1.752	1.750	1.775	1.52	1.56	1.554	1.555
H-13	5.475	5.508	5.537	5.52	~5.55	5.561	5.572
H-14	5.563	5.583	5.594	5.56	~5.58	5.595	5.603
H-15	4.053	4.101	4.130	4.05	4.17	4.157	4.164

[a] All shift values are based on δ(H-20) = 0.890. [b] Data of Conover & Fried (1974), reanalyzed in the light of assignments based on high-field data in some instances. All other data are from the present study. [c] These methylenes are nonequivalent but $\Delta\delta_{AB} \lesssim 0.01$.

and δ values were assigned for all resonances. The δ values were redetermined after each of a series of sequential additions of $Pr(NO_3)_3/D_2O$ producing Pr/La ratios from 0.0 to 0.6.

Results

Resonance Assignments for $PGF_2\alpha$ Free Acid Analogues. Previous ^1H and ^{13}C NMR studies of $PGF_2\alpha$ in D_2O (Conover & Fried, 1974) indicated increasing intermolecular association in the 20–200 mM range. This study was not extended to lower concentration to ascertain whether 20 mM was at or below the association limit. Therefore, we determined spectra at 2, 5, 10, and 20 mM and for comparison purposes also recorded spectra of $PGF_2\alpha$ free acid and ester in $CDCl_3$. The chemical shifts of selected, readily assigned protons appear in Table I. In order to allow direct comparison with the earlier work, the terminal Me resonance was used as the standard (δ = 0.890).

Chemical shift values for the ester were not (±0.01 ppm) concentration dependent, but those for the free acid in $CDCl_3$ were. The latter may reflect varying residual water content and equilibria between the acid dimer and oligomeric forms. Turning to aqueous solution data, we find that the dilution-induced shift trends observed by Conover & Fried (1974) continue to the 10 mM level but that further dilution to 5 or 2 mM does not produce significant ($\Delta\delta < 0.014$) changes for proton signals whose resonance position can be assigned by first-order analysis. We therefore conclude, for $PGF_2\alpha$, that aggregate formation at pH 8–9 begins to contribute significantly at concentrations between 10 and 20 mM. Recent studies of proton resonance longitudinal relaxation rates in D_2O at 2, 5, and 10 mM confirm the lack of association in this concentration range (Andersen et al., 1984a). For the less polar methylated analogues the lower limit for association may be as little as 5 mM.

At 500 MHz the aqueous medium spectrum of $PGF_2\alpha$ still displays significant resonance overlap (see Figure 3), but all resonances other than the broad singlet at δ 1.29 (due to the methylenes at C-17 → C-19) can be unambiguously assigned to individual protons by a combination of spin–spin decoupling and ΔNOE spectra. The complete sequence of experiments establishing connectivity and stereochemistry will not be detailed here.[4] Some of the key ΔNOE spectra are collected in Figure 4. The two nonequivalent hydrogens at C-10 were

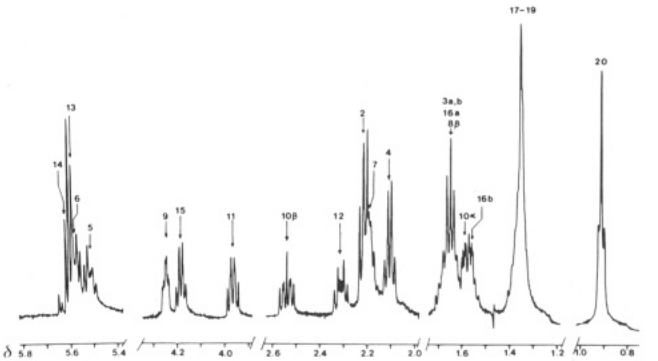

FIGURE 3: 500-MHz FT NMR spectrum of 2 mM $PGF_2\alpha/D_2O$ (20 mM K_2DPO_4, nominal pH 9). This 32K spectrum was obtained in 30 min (200 pulses). Expanded portions of a similar spectrum (from a 10 mM solution) appear as the topmost trace in Figure 4. Note the concentration- and pH-induced change in the relative positions of the H-2 and H-7 resonances.

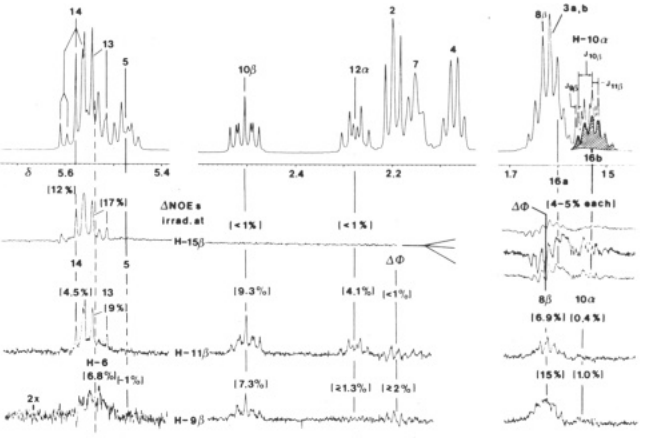

FIGURE 4: ΔNOE spectra (at 500 MHz) of 10 mM $PGF_2\alpha$ at ca. pH 8. The top trace shows the control spectrum; the hatched area is resonance H-16b hidden under H-10α. The lower traces are ΔNOE spectra (32 cycles of 8 pulses on- and off-resonance, 75-min accumulation per specific irradiation site) due to irradiation at H-15β, -11β, and -9β, respectively. NOE quantitation is from the integral traces (not shown). Δφ indicates phase shift anomalies or SPT effects which produce no net integrated intensity.

readily detected by the decoupling experiments irradiating at H-9β and -11β. The ΔNOE integrals establish that the downfield member of the pair is cis to H9β and -11β (see Figure 4). The resulting assignments of H-10α and H-10β are the reverse of those reported by Conover & Fried (1974). Our assignment is in agreement with expectations based on the "syn upfield" rule as delineated by Anteunis & Danneels (1975). The δ 1.6–1.7 region was particularly cluttered and contained the H-8β resonance (see Figure 4) which bore

[4] The sequence for each analogues begins with defining H-15 as that CHOH signal that has a *J* coupling to an olefinic H (H-14); this serves to identify H-13, which reveals H-12, which reveals H-11. The remaining CHOH is thus H-9β which displays an NOE with one of the remaining olefinic resonances (thus assigned to H-6). The complete sequence and logic for each analogue can be found in Lin (1983), which also contains a complete set of δ and *J* values for each analogue. The 16(*R*)- and 16(*S*)-methyl assignments are discussed in a later section.

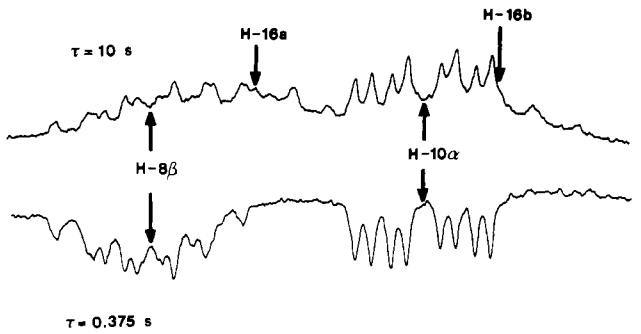

FIGURE 5: δ 1.45–1.7 region of two spectra (at 303 K) from inversion recovery experiments conducted on 5 mM $PGF_2\alpha$-*3,3,4,4-d*$_4$/D_2O (20 mM phosphate pH ≈ 8.6), showing the elimination of the signals due to the C-16 methylene. The partially relaxed spectrum required 2500 pulses (vs. 100 for the τ = 10 s scan): τ_{null} for H-8 and H-10α was found to be 0.49 s.

Table II: Chemical Shifts and Splittings for 2 mM $PGF_2\alpha$ (and Analogues):[a] D_2O (pH ~9)

proton	chemical shift[b]	coupling constants (Hz)
H-2	2.160	$J_{2,3}$ = 7.7
H-3	1.61[a]	$J_{3,4}$ = 7.1
H-4	2.048[a]	$J_{4,5}$ = 7.1
H-5	5.459[a]	$J_{5,6}$ = 10.8
H-6	5.522[a]	$J_{6,7} \gtrsim 8$, $\lesssim 5$
H-7a, -7b	2.14[a]	$J_{7,8} \gtrsim 8.3$, $J_{7',8} \lesssim 6.2$
H-8	1.62[a]	$J_{8,9}$ = 5.6, $J_{8,12}$ = 11.6
H-9	4.192[a]	$J_{9,10\alpha}$ = 2.5, $J_{9,10\beta}$ = 6.2
H-10α	1.517[a]	$J_{10\alpha,11}$ = 6.0, $J_{10\alpha,10\beta}$ = 14.7
H-10β	2.482[a]	$J_{10\beta,11}$ = 8.5
H-11	3.908[a]	$J_{11,12}$ = 7.9
H-12	2.254[a]	$J_{12,13}$ = 7.7
H-13	5.534[a]	$J_{13,14}$ = 15.4
H-14	5.565[c]	$J_{14,15}$ = 7.1
H-15	4.126	$J_{15,16}$ = 7.0
H-16a	1.60	$J_{16a,16b}$ ~ 13
H-16b	1.50	$J_{16,17}$ ~ 7.5
H-17, -18, -19	1.287	
H-20	0.852	$J_{19,20}$ = 6.9

[a] In the three analogues examined these resonances appeared within ±0.02 ppm of the value for unsubstituted racemic $PGF_2\alpha$. [b] On the basis of DSS = 0.000, add 0.015 ppm to obtain standard shift values. [c] Shifted 0.07–0.09 ppm downfield in the three analogues.

coupling information essential for elucidating the cyclopentane ring conformation. In order to reduce the signal overlap (and to confirm the H-3a,b assignment), spectra of $PGF_2\alpha$-*3,3,4,4-d*$_4$ were recorded. By the appropriate choice of τ in an inversion recovery experiment the C-16 methylene signals could be eliminated (see Figure 5), allowing the direct analysis of coupling associated with H-8β. The complete assignment of the 2 mM, pH 9, spectrum of $PGF_2\alpha$ appears in Table II.

Three analogues (15-*epi*-$PGF_2\alpha$, 17,17-Me_2-$PGF_2\alpha$, and 16,16-Me_2-$PGF_2\alpha$) were also studied at 2–5 mM in phosphate-buffered D_2O. Similar decoupling and ΔNOE spectra provided complete resonance assignments.[4] The chemical shifts for all hydrogens were, with the exceptions noted, within ±0.02 ppm of the values appearing in Table II. The H-2 resonance varied, presumably due to minor pH differences. The major changes were at the H-15 resonance: δ 4.155 (15-epi), 4.255 (17,17-Me_2), and 3.859 (16,16-Me_2). The methylated analogues each showed two diastereotopic Me singles resonances: δ 0.901 and 0.896 (17-Me_2); 0.883 [16(*S*)-Me] and 0.846 [(16(*R*)-Me].[4] Resonances due to hydrogens vicinal to the CMe_2 groups were shifted upfield: 0.26 ppm for H-15 of 16,16-Me_2-$F_2\alpha$ and 0.08–0.10 ppm for thw C-16 methylene protons of 17,17-Me_2-$F_2\alpha$. NOE data for aqueous solution spectra appear in Table III.

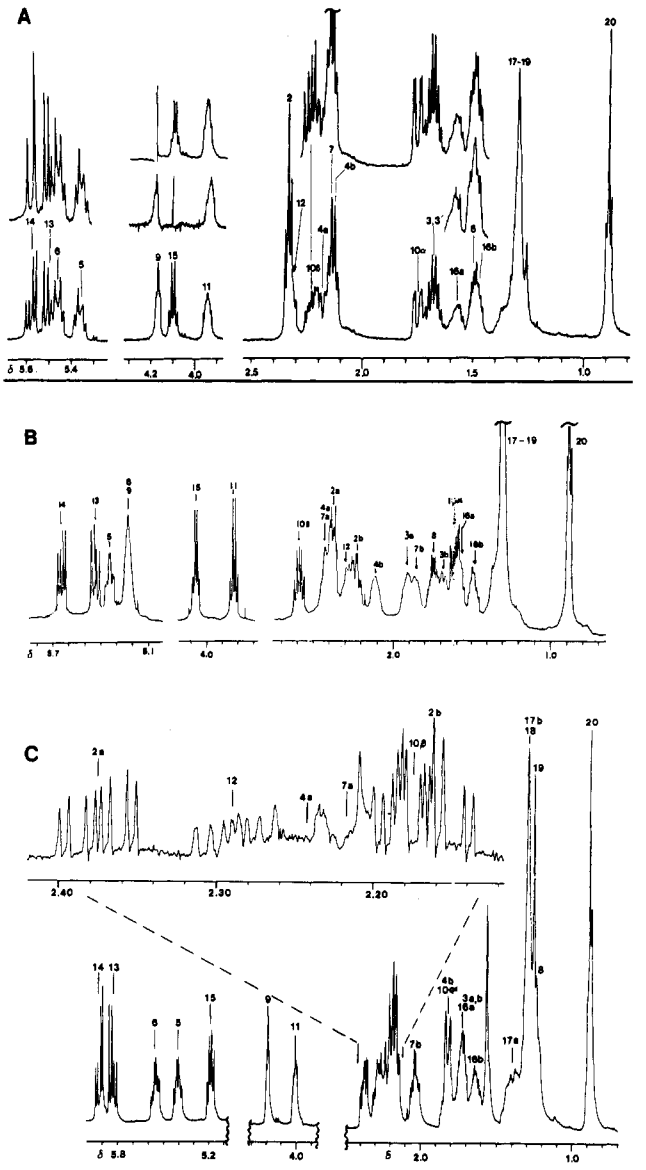

FIGURE 6: NMR spectra of $PGF_2\alpha$ and derivatives in $CDCl_3$. (A) *rac*-$PGF_2\alpha$ (20 mM) + trace D_2O. The upper partial traces show key homonuclear decoupling experiments irradiating at H-15 and H-9. (B) The spectrum of $PGF_2\alpha$-1,9-olide. (C) The full-scale (resolution not enhanced) spectrum of $PGF_2\alpha$-1,15-olide. The expanded section is a resolution-enhanced trace.

Resonance Assignments for $PGF_2\alpha$ Esters and Lactones in $CDCl_3$ Solution. $PGF_2\alpha$ and its methyl ester display similar spectra in $CDCl_3$ with no chemical shift differences greater than 0.05 ppm. The $CDCl_3$ spectra (see Figure 6) are notably different than the spectra recorded for aqueous media with Δδ values as great as 0.4 ppm. Surprisingly large diastereotopic Δδ's for the methylenes at C-3, C-4, and C-7 were observed (these CH_2 groups had been nearly isochronous in the spectra of $PGF_2\alpha$ and its analogues in D_2O). Such nonequivalence in a $PGE_2/CDCl_3$ spectrum has previously been cited as due to restriction of free rotation and indicative of a hairpin conformation (Kotovych et al., 1980b). Because of the questions concerning side-chain motions we also examined medium- and large-ring lactonic forms of $PGF_2\alpha$ that would be expected to display restricted side-chain motion. The richly detailed spectra of $PGF_2\alpha$-1,9-olide and -1,15-olide are compared to the uncyclized form in Figure 6.

The C-8 → C-16 bound proton resonances labeled in Figure 6 were assigned by the same sequence of decoupling experiments employed for aqueous $PGF_2\alpha$. The nonequivalency of

Table III: NOE Quantitation Matrix: ΔNOE Integrals from D_2O Solution Studies of $PGF_2\alpha$ Analogues

	H-8	H-9	H-10α	H-10β	H-11	H-12	H-13	H-14	H-15	H-16a	H-16b	H-17 → H-19	other
16,16-Me_2	2.2		≲0.6	4.8	−100	2.0	5.6	1.7	−10				1.4 [16(*R*)-Me]
						8.5	−12	−100	2.1			2.1	2.1 [16(*R*)-Me]
					−13		9.2	2.5	−100				2.6 [16(*S*)-Me]
													1.6 [16(*R*)-Me]
17,17-Me_2	3.4		0.8	4.3	−100	2.2	4.3	1.3					
		−6.2					7.4	3.0	−100	1.6	1.6		1.2 (17b-Me)
													2.4 (H-18 + H-19)
$PGF_2\alpha$	15	−100	1.0	7.3		≲1.4							1 (H-5)
													6.8 (H-6)
	6.9		0.4	9.3	−100	4.1	9.0	4.2					
	≲2			<1		<1	17	12	−100	4	4		

all of the methylene units in the large rings of the lactones facilitated the assignment process, and sequential spin decoupling experiments gave an unambiguous determination of connectivity. In both lactones one hydrogen each at carbons 2, 3, 4, and 7 displayed a three bond scalar coupling in the 9.5–12.7-Hz range, suggesting vicinal interactions locked in either an antiperiplanar or eclipsed disposition. ΔNOE spectra distinguished between these two possibilities in each case; thus, lactone ring conformations can be postulated. The ΔNOE spectra integrals for both macrolides are collected in Table IV. In the case of the 1,9-olide, the conformation elucidation sequence begins with the observation that H-8β shows a substantial NOE with that C-7 hydrogen [H-7(*S*)] with which it does not display a large scalar coupling. ΔNOE spectra [irradiated H-7(*S*)] demonstrate that H-7(*S*) has substantial dipolar cross-relaxation with both H-13 and H-14 in the other side chain. Two views of a conformation consistent with these observations (and the coupling constants listed in the figure legend) appear as panel A of Figure 7. The substantial H-5/H-3(*S*) (upfield of pair) cross-relaxation serves as a confirmation of the C-2 → C-5 ring fragment conformation.

In the case of the 1,15-olide, the analysis was complicated by the overlap of one each of the C-4 and C-7 methylene hydrogens and by the smaller value of $\Delta\delta(3R,3S)$ in this analogue. Figure 7 (panel B) illustrates a macrolide ring conformation consistent with the coupling and NOE data. In support of this hypothesis we note the axial C-2 hydrogen (H-2(*R*), downfield of pair) transanular NOEs with both H-8 and H-13 and the other NOEs underlined in Table IV. The conformation assignment in the case of the 1,9-olide is nearly conclusive, and studies of the field dependence of T_1 data (Andersen et al., 1984a) indicate that a single rigid conformer describes this molecule adequately. The 1,15-olide assignment is less secure, and phase sensitive NOESY spectra will be obtained for both substances to substantiate these hypotheses.

Cyclopentane Conformational Preferences. The most direct assessment of the portion of the five-membered ring pseudorotational itinerary (Figure 2) occupied by each analogue comes from a comparison of the observed coupling constants with calculated values based on expectation dihedral angles using a modified Karplus equation. Two coupling constants serve to limit the search. In all substances studied $J_{8\beta,12\alpha}$ is 10–11.8 Hz (approaching values associated with an antiperiplanar relationship) and $J_{9\beta,10\alpha}$ is less than 3.5 Hz (ϕ = 55–115°). These two features co-occur over only a small portion of the complete itinerary. As a result the conformational preferences of all of the analogues can be placed in the C_s–C12$^\alpha$ → C_s–C9$^\alpha$ region. To within experimental error the three $PGF_2\alpha$ analogues examined in D_2O solution display the same coupling constants about the cyclopentane ring (Table V). Significant changes appear only in $J_{12,13}$ which reflects the disposition of the ω side chain, the site of alteration in the

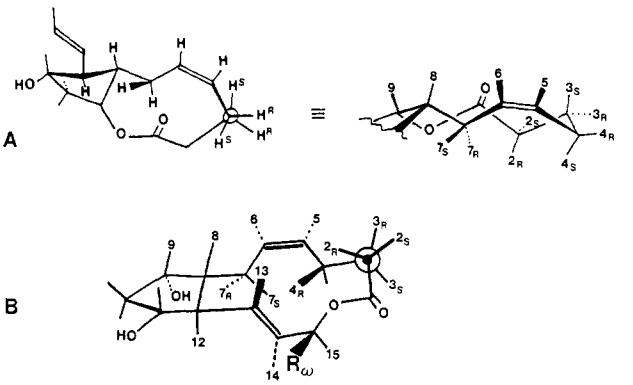

FIGURE 7: Macrolide ring conformations. (A) Two views of the 10-membered ring conformation assigned to $PGF_2\alpha$-1,9-olide. The *R*/*S* designations correlate with Figure 6 (panel B) assignments as follows: 2.372 (2a = *S*), 2.236 (2b = *R*), 1.907 (3a = *R*), 1.682 (3b = *S*), 2.41 (4a = *S*), 2.111 (4b = *R*), 5.343 (5), 5.22 (6), 2.41 (7a = *R*), 1.855 (7b = *S*). Key *J* values not reported in other parts of this article are 3.9 (2*S*,3*R*; 2*S*,3*S*), 5.12 (2*R*,3*R*), 12.7 (2*R*,3*S*), ≲1.5 (3*S*,4*R*), 11 (5,4*S*), 4.9 (5,4*R*), and 1.47 Hz (5,7*S*). (B) The 13-membered ring conformation proposed for $PGF_2\alpha$-1,15-olide. The *R*/*S* designations correlate with the assignments depicted in Figure 6 (panel C) as follows: δ 2.376 (2a = *R*), 2.162 (2b = *S*), ≈1.73 (H-3*R* and -3*S*), 2.24 (4a = *R*), 1.82 (4b = *S*), ≈2.22 (7a = *S*), 2.04 (7b = *R*), 5.407 (5), 5.556 (6), 1.237 (8), 5.829 (13), and 5.919 (14). Key *J* values not recorded elsewhere: 13.12 (2*R*,*S*), 8.24 (2*R*,3*S*), 2.75 (2*R*,3*R*), 3.05 (2*S*,3*S*), 10.08 (2*S*,3*R*), 9.46 (4*R*,5), 6.1 (4*S*,5), 10.99 (6,7*S*), 5.18 (6,7*R*), 14.7 (7*R*,*S*), 1.83 (8,7*S*), 10.38 (8,7*R*), 6.41 (15,16a), and 8.24 Hz (15,16b).

analogues. In contrast, $PGF_2\alpha$ (or its methyl ester in $CDCl_3$) in $CDCl_3$ displays a radically different set of *J* values, and each position of lactone closure produces changes in the cyclopentane conformational preference. The 1,9-olide closure causes the greater deviation (vs. $PGF_2\alpha$ methyl ester in $CDCl_3$), with the more accommodating 13-membered ring of the 1,15-olide leaving the cyclopentane conformation of $PGF_2\alpha$ methyl ester only slightly altered. The fit between pseudorotamer models and the observed *J* values appears in Table IX and is detailed under Discussion.

The ΔNOE integral spectra provide another basis for assigning the cyclopentane conformation. The 11β hydrogen cross-relaxes with all of its vicinal neighbors and with three hydrogens that are four or more bonds removed (Table VI). The 11β/8β through space interaction should be a sensitive measure of ring conformation. In the C_2^-–C_9 form it approximates a 1,3-cis diaxial cyclohexane interaction, and cross-relaxation should be maximal. The 11β/12α interaction would be maximal at C_s–C8$^\beta$. The data in Table VI confirm the similarity of $PGF_2\alpha$ (D_2O) and $PGF_2\alpha$-1,9-olide which was suggested by the cyclopentane vicinal coupling constant comparison. On the basis of the NOE data the 1,9-olide would be placed at C_s–C12$^\alpha$/C_2^+–C10 with $PGF_2\alpha$ and then its substituted analogue displaced toward C_s–C8$^\beta$ and C_2^-–C11.

Table IV: NOE Quantitation Matrices (ΔNOE Integrals) for $PGF_2\alpha$-1,9-olide and -1,15-olide[a]

compound	H-2a	H-2b	H-3a	H-3b	H-4a	H-4b	H-5	H-6	H-7a	H-7b	H-8	H-9	H-10α	H-10β	H-11	H-12	H-13	H-14	H-15	H-16a	H-16b	H-17–19
1,9-olide	1.5	1.6	−100	−7	*b*	−0.5	2.5	5.8	6[b]	−100	−7						2.7	1.6				
	4.0	<0.5	−2.2	−100	<0.2	0.8	5.0	*c*	<0.2	−1.1	−60	4.7[c]		2.0								
			0.8	2.3	0.8	2.0	−100	−26			1.0	−26										
							−14	−100	0.8	2.2	10	−100	1.0	4.5								
				−12				10		−8.5	−100	10			4.2	1.6	6.5	1.1				
											3.0		<1	5.4	−100	1.3	4.2	1.0				
								<0.2	<0.2					<0.3		<0.4	7.8	2.5	−100	2.4	1.9	7.4
1,15-olide	−100	21		2.0		1.8	1.2		<0.2	~0.9	2.4				1.0	−12	2.5					
				1.2				8			1.0											
					0.8	3.0	−100	−100	<0.5	3.8	2.4	2.3										
					<0.5	<0.5	9				2.7		1.0	4.0	−100	2.5	3.2	1.1				
															2.7	7.2	−20	−100	7			
																	2.4	6	−100	2	2	7

[a] In the designation (3a, 3b, etc.) of diastereotopic methylene resonances, a always refers to the downfield resonances. See text and Figures for *RS* assignments. [b] H-4a+7a are an overlapping multiplet in the 1,9-olide spectrum; the NOE observed is presumably of 7a due to irradiation at 7b. [c] H-6+9 unresolved; the NOE is attributed to 8 → 9.

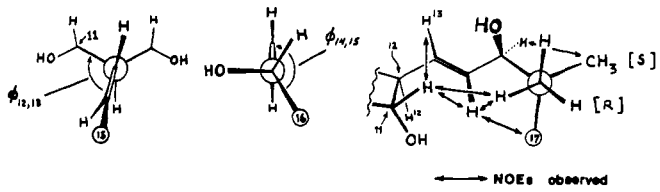

FIGURE 8: Conformational models for the C12–C17 fragment of $PGF_2\alpha$ analogues in aqueous media.

The relatively smaller H-8β (←H-11) enhancements observed for $PGF_2\alpha$-1,15-olide and $PGF_2\alpha$ methyl ester in $CDCl_3$ suggest a further progression toward the C_s–$C9^{\alpha}$ conformer.

Side-Chain Disposition in Nonlactonic Analogues. Secure assignment of side-chain conformational features in the case of the monocyclic compounds can only proceed outward from the cyclopentane ring to the reach of overlapping NOEs beginning with irradiations at cyclopentane hydrogen sites. As seen in Table VI, irradiation at H-11 produces readily measurable NOE enhancements at H-13 and H-14, and these same hydrogens also cross-relax with H-15. These NOE ratios serve as a sensitive measure of the orientation of the trans $\Delta^{13,14}$ unit relative to H-15 (and by inference to C-16). The values of $J_{12,13}$ and $J_{14,15}$ are additional parameters bearing on the same conformational feature. The pertinent data appear in Table VII. The ΔNOE ratio of H-14 to H-13, upon irradiation at H-11β, decreases as the value of $J_{12,13}$ increases (see Table VII). With the exception of 15-*epi*-$PGF_2\alpha$ and $PGF_2\alpha$-1,15-olide, in which the orientations are forced to be different, the size of $J_{14,15}$ and the relative dominance of dipolar cross-relaxation to H-13 (rather than H-14) also correlate. The large values of $f_{14}[11\beta]$ and $f_{13}[15]$ can be rationalized by a model shown in Figure 8.

Upon closer examination the ΔNOE data of 16,16-Me_2-$PGF_2\alpha$ provided information about the C-15/C-16 rotameric preference and made the assignments of the two diastereotopic methyl groups possible. When H-15 was irradiated, the downfield methyl showed a somewhat larger enhancement. The saturation of either H-11 or H-14 showed a significant NOE only on the upfield methyl signal. These imply that the upfield methyl group is close to H-11 and H-14 but positioned anti to H-15. Inspection of molecular models suggests the conformation from C-12 to C-16 as shown in Figure 8. Therefore, the upfield signal was assigned to the C-16 (*pro-R*)-methyl group and the downfield one was assigned to the (*pro-S*)-methyl group. This assignment of the two methyl signals is also consistent with the syn upfield rule.

Lanthanide Shift Data. Lanthanide ions, as relaxation and pseudocontact shift reagents, have enjoyed a period of great popularity as structure elucidation probes (Inagaki & Miyazawa, 1981). The method suited our needs well due to the high affinity and specificity of Ln(III)–carboxylate binding in aqueous media near neutrality (pH 6–9). The chemical shift induced upon addition of a paramagnetic Ln species such as Pr(III) can be factored as

$$\Delta\delta(\mathrm{Pr}) = \Delta\delta_{pc} + \Delta\delta_{cf} + \Delta\delta_{bulk}$$

with $\Delta\delta_{bulk}$ representing the nonintramolecular interactions on both the free carboxylate and Pr complex. The pseudocontact term, $\Delta\delta_{pc}$, is the one required for structure correlation. The diagmagnetic shift terms associated with complex formation ($\Delta\delta_{cf}$) are typically separately assessed by examining a stoichiometrically formed, isomorphous, diamagnetic complex such as La(III).

We chose to modify a procedure of Elgavish & Reuben (1976) so as to obtain relative $\Delta\delta_{pc}$ values directly. The prostaglandin, excess EDTA, a stoichiometric quantity of

Table V: Coupling Constants (in Hertz) for $PGF_2\alpha$ Analogues

	$PGF_2\alpha$ and its analogues in D_2O solutions (2 mM)				$PGF_2\alpha$ (5 mM) and its esters (10 mM) in $CDCl_3$			
coupling constants	16,16-Me_2 $PGF_2\alpha$	17,17-Me_2 $PGF_2\alpha$	15-epi-$PGF_2\alpha$	$PGF_2\alpha$	free acid	Me ester	1,9-olide	1,15-olide
$J_{8,9}$	5.35	5.35	5.4	5.6	4.2	4.4	6.84	5.19
$J_{8,12}$	11.6	11.7	11.8	11.6	10.0	10.7	11.7	11.29
$J_{9,10\alpha}$	2.7	2.6	2.6	2.5	0.9	1.3	3.41	0.9
$J_{9,10\beta}$	6.35	6.1	6.2	6.2	5.4	4.9	7.3	4.27
$J_{10\alpha,11}$	6.1	6.1	6.1	6.0	2.4	3.6	8.05	2.75
$J_{10\beta,11}$	8.55	8.55	8.4	8.5	8.1	8.0	8.3	7.32
$J_{11,12}$	7.9	8.05	7.8	7.9	5.5	5.4	8.3	4.58
$J_{12,13}$	9.3	8.7	8.1	7.7	8.1	8.7	9.0	8.85
$J_{14,15}$	8.54	8.06	6.3	7.1	6.2	7.2	7.32	6.41
$J_{7a,8}$				$\gtrsim$8.3			11.7	1.83
$J_{7b,8}$				$\lesssim$6.2			4.64	10.4

Table VI: Dipolar Relaxation due to H-11

	fraction (due to H-11β) of R_{1D} at				
compound	H-8β	H-10β	H-12α[a]	H-13	H-14
$PGF_2\alpha$-1,9-olide	2.3	4.1	1.0	3.2	0.8
$PGF_2\alpha$ (D_2O)	1.7	2.3	1.0	2.2	1.0
17,17-Me_2-$F_2\alpha$	1.55	2.0	1.0	2.0	0.6
16,16-Me_2-$F_2\alpha$	1.15	2.4	1.0	2.8	0.85
$PGF_2\alpha$ methyl ester ($CDCl_3$)	0.95	2.1	1.0	2.05	0.7
$PGF_2\alpha$-1,15-olide	1.1	1.6	1.0	1.3	0.44

[a] The ΔNOE integral at H-12α was set equal to 1.00 for standardization for each compound. Relative steady-state NOEs cannot be used quantitatively to obtain distances.

Table VII: NMR Parameters Pertaining to the Conformational Disposition of the Δ^{13}-Olefin Unit

compound	ΔNOE(H-14)/ ΔNOE(H-13) (irrad H-11)	$J_{12,13}$	ΔNOE(H-14)/ ΔNOE(H-13) (irrad H-15)	$J_{14,15}$
$PGF_2\alpha$ (D_2O)	0.47	7.7	0.7	7.1
16,16-Me_2-$PGF_2\alpha$ (D_2O)	0.30	9.3	0.27	8.54
17,17-Me_2-$PGF_2\alpha$ (D_2O)	0.30	8.7	0.40	8.06
15-*epi*-$PGF_2\alpha$ (D_2O)			0.43	6.3
$PGF_2\alpha$-1,15-olide ($CDCl_3$)	0.34	8.85	2.5	6.41
$PGF_2\alpha$ methyl ester ($CDCl_3$)	0.33	8.72	0.50	7.18
$PGF_2\alpha$-1,9-olide ($CDCl_3$)	0.26	9.0	0.32	7.32

$La(NO_3)_3$, and DSS as a shift standard were dissolved in phosphate-buffered D_2O (pH 6.5–9). The initial spectra showed no change in conformation (all J values ± 0.15 Hz of value in the absence of La). A graph of δ vs. added Pr-(EDTA)$^{1-}$ (0.0–0.11 equiv relative to La) provides (rel $-\Delta\delta_{pc})_i$ as the slope. When δ values are referenced to internal DSS, which also has an anionic head but binds Pr much less avidly than either the PG or EDTA, the $\Delta\delta_{bulk}$ term is eliminated. The $\Delta\delta_{cf}$ term remains constant since the Ln:PG ratio changes less than 16% during the experiment[5] and thus does not contribute to the slope. Relative $\Delta\delta_{pc}$(Pr) values obtained in this way appear as the first four columns of Table VIII. The final column of Table VIII shows additional Pr(III) shift ratios for free fatty acids determined by a different protocol (Leovey & Andersen, 1975b).

For any single conformer of a Ln complex one may assume

$$(\Delta\delta_{pc})_i/(\Delta\delta_{pc})_j = \frac{(3\cos^2\theta_i - 1)r_j^3}{(3\cos^2\theta_j - 1)r_i^3}$$

for any two hydrogens (i, j) at different orientations relative to the Ln center. The use of the McConnell–Robertson equation is valid when the magnetic axis is collinear with the Ln-donor bond. As applied to carboxylates this is equivalent to placing the Ln on the bisector of the carboxylate, collinear with the C-1,2 C–C bond at ca. 0.50 nm from C-2 (Perly & Chachaty, 1982). This assumption is supported by numerous studies of carboxylates and amino acids [for example, see the review of Inagaki & Miyazawa (1981)]. The $\Delta\delta_{pc}$ values for H-2 → H-6 for the $PGF_2\alpha$ analogues are in complete agreement with those seen in straight-chain fatty acids, suggesting that no unusual conformational constraints are present in the terminal portion of the α chain. Due to the uncertainty with regard to the placement of the $-CO_2Pr$ center relative to the remaining portions of the molecule, we have to ignore the angular factor and assume only an approximate inverse distance relationship. What is clear is that, although the carboxyl-bearing chain emanates from the α-face of the cyclopentane ring, the carboxylate terminus is above (β to) the ring. This is most clearly evident in the comparison of $\Delta\delta_{pc}$ for 10α- and 10β-H but is confirmed in other comparisons including the 16a(*S*)-Me/16b(*R*)-Me values for 16,16-Me_2-$PGF_2\alpha$ (see Figure 8). The 10α hydrogen is clearly the most remote point from the carboxylate: the Δ^{13}-en-15-ol and terminal methyl are significantly closer to the Pr center. The $\Delta\delta_{pc}$ values for the dimethylated analogues are virtually the same as those for natural $PGF_2\alpha$; if any change is indicated, the data suggest a greater α/ω distance for the 16,16-dimethyl species (Table VIII). A shortening, due to C-16 dimethylation, of the C-20/C-1 vector had been anticipated (Andersen et al., 1976, 1981c).

Discussion

Contrasts between Solution- and Solid-State Cyclopentane Conformational Preferences. X-ray crystal structures due to the Medical Foundation of Buffalo group (DeTitta et al., 1980, and references cited therein) provide the best data on the pseudorotational preferences of the cyclopentane ring in prostaglandins. For prostaglandins lacking sp^2 centers in the five-membered ring, at least four pseudorotameric forms are represented, with the C_s–C9$^\alpha$ form being the most common. Conover & Fried (1974) concluded that this same conformer predominated in aqueous solution on the basis of NMR data; however, key cyclopentane vicinal coupling constants were assigned incorrectly due to the reversed assignment for the C-10 methylene resonances. We have calculated J values for four conformation observed in the solid state and for idealized representations of seven conformers and compared these to the observed splittings for $PGF_2\alpha$ (in two solvents) and its two lactonic forms (see Table IX).

The ΔNOE integrals for $PGF_2\alpha$ and the 1,15-olide in $CDCl_3$ solution were consistent with the C_s–C9$^\alpha$ conformer (see

[5] The percent $-CO_2Ln$ complex changes even less due to the competition of excess EDTA for Ln(III) ions.

Table VIII: Pr(III)-Induced Changes in Chemical Shifts for $PGF_2\alpha$ Analogues and Straight-Chain Free Fatty Acids (FFA)

	relative $\Delta\delta_{pc}$(Pr)				
	5 mM acid in D_2O at "pH 6.2" + Pr(EDTA)$^{1-}$				acid + $Pr(NO_3)_3$ in 2:1 D_2O–Bu^{t}OD, NaOH titration, for FFA
	$PGF_2\alpha$	16,16-Me_2 $PGF_2\alpha$	17,17-Me_2 $PGF_2\alpha$	FFA	
H-2	100	100	100	100	100
H-3	58	58	60	57	57.8 ± 0.9
H-4	34	34	34	35	35 ± 1
H-5	18	21	20	20	21.8 ± 1.3
H-6	11.6	10.6	10.2	10	12 ± 2
H-7a	14.0	10.5	12.6		7.8 ± 0.4
H-7b	12.4				
H-8β	8.1		7.9	2.8	5.8 ± 0.8
H-9β	4.5	4.3	5.2		$\lesssim$3.8 ± 1.0
H-10α	1.1	1.1	<1.5		
H-10β	1.85	1.54	1.97		$\lesssim$2.6 ± 0.5
H-11β	2.5	2.3	2.6		
H-12α	3.7		4.2		
H-13	4.65	4.6	5.1		
H-14	4.1	4.0	4.2		
H-15	3.4	3.1	3.7		
H-16a	3.3		3.9[a]		
H-16b	4.0		3.0[a]		
Me-16a		2.9			
Me-16b		3.92			
Me-17a			3.7		
Me-17b			3.3		
H-17 to H-19	3.9	3.15			$\lesssim$1.2 ± 0.5
H-18, -19			3.6		
H-20	2.52	2.13	2.47		

[a] Note that the high-frequency (a) and low-frequency (b) resonances for the C-16 methylene show opposite LIS values in the methylated analogue.

above). The full coupling constant comparison in Table IX confirms this: the chloroform solution value for $PGF_2\alpha$ free acid displays an almost perfect fit to the C_s–C9$^\alpha$ form observed in the crystal structure of the Tris salt of $PGF_2\alpha$ (molecule A, Figure 1). On the basis of the measure of fit analysis, $PGF_2\alpha$-1,9-olide is best approximated as a mixture of the C_s–C12$^\alpha$ and C_2^+–C10 forms, with the latter making the major contribution. For the aqueous solution data, the C_s–C8$^\beta$ pseudorotamer provides the best single fit. However, this analysis should not be taken to indicate that adjacent forms (such as C_2^+–C10 and C_2^-C11) do not contribute, nor do the data demand the existence of large barriers to pseudorotation within the limited itinerary shown in Table IX. However, it would appear that in each system the cyclopentane ring conformation can be adequately modeled as either a single pseudorotamer or at most a mixture for two or three closely related conformers with one making a dominant contribution. On the basis of the coupling constants and NOE data the systems studied are placed within pseudorotational itinerary as shown.

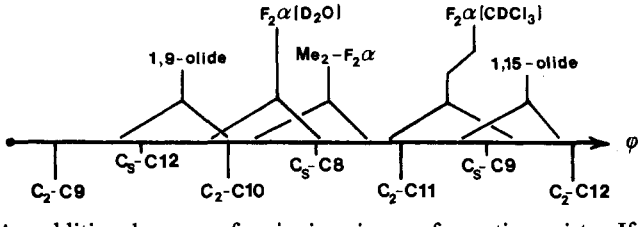

An additional means of assigning ring conformation exists. If the chemical shift nonequivalence of the C-10 methylene protons is assumed to be due only to near neighbor effects, the relative spatial disposition of β (and to a lesser extent γ) substituents, particularly the two vicinal hydroxyl groups, the ring conformation can be calculated. The work of Anteunis & Danneels (1975) provides a tested relationship between dihedral angle and shielding parameters for both the hydroxyl and methyl group. The solid-line plot in Figure 9 is the expectation value for the $\Delta\delta(10\beta/10\alpha)$ contribution of syn shielding due to the two hydroxyls through a pseudorotational itinerary. The dashed line includes β- and γ-alkyl effects as well, assuming the shielding parameters of the methyl group apply. Either analysis suggests maximal relative upfield shift

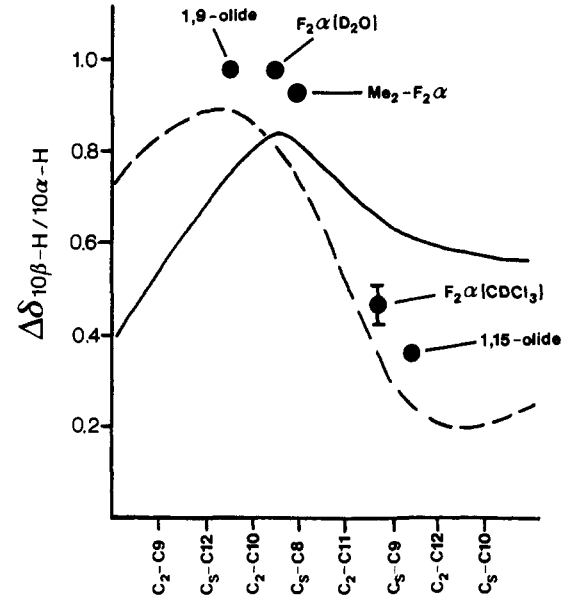

FIGURE 9: Predicted vs. observed chemical shift differences for the C10 methylene: $\Delta\delta(=\delta_{10\beta} - \delta_{10\alpha})$ is plotted vs. the pseudorotameric position. The solid line shows the calculated effect due to the 9α- and 11α-hydroxyls based on additivity of the shielding effects. The dashed line includes a treatment of C8, C12, C7, and C13 as β and γ substituents, respectively. The shielding dihedral angle dependencies employed are those for OH and CH_3 from the work of Anteunis & Danneels (1975). The Hendrickson (1961) models of C_s and C_2 forms of cyclopentane were used for all calculations of dihedral angles (see notes for Table IX). Solid circles are observed values placed at the point along the itinerary indicated by NOE and scalar coupling analysis.

Table IX: Measure of Fit Comparisons between Observed and Calculated[a] Coupling Constants Based on Idealized[b] and Solid-State Conformations[c] of PGF Species

pseudo-rotamer (basis)	$\sum(\Delta J)^2$[e]			
	$PGF_2\alpha$ free acid in		1,15-olide in $CDCl_3$	1,9-olide in $CDCl_3$
	D_2O	$CDCl_3$		
C_2–C9 (ideal)	77	>100	>100	32.8
C_s–C12 (ideal)	36.1	>100	>100	13.2, 16.8
C_s–C12 ($PGF_2\beta$)[d]	36.6	113	>100	13.3
C_2–C10 (ideal)	14.4, 15.8	65.2	>90	8.4, 10.9
C_2–C10 ($PGF_1\beta$)[d]	20.9	82.6	96	9.8
C_s–C8 (ideal)	7.6, 8.8	28.4, 29.5	39.6, 41.5	18.5, 23.0
C_s–C8 ($PGF_2\alpha$, *B*)	10.5	19.4	32.5	19.7
C_2–C11 (ideal)	15.6, 16.8	6.3, 5.3	10.9, 12.1	40.4, 38.2
C_s–C9 ($PGF_2\alpha$, *A*)	28.6	2.5	6.5	55.5
C_s–C9 (ideal)	38.4	4.7, 3.6	8.7, 4.9	70
C_2–C12 (ideal)	77	24.7, 19.7	26.5, 23.6	>100

[a] $^3J = (7.0 - 1.2\cos\phi + 5.6\cos 2\phi)(1 - 0.1\sum\Delta\chi_i)$ where $\sum\Delta\chi_i$ is the sum of the electronegativity differences between substituents on the ethane fragment and hydrogen. Durette & Horton (1971) used a similar relationship ($A = 7.8$, $B = -1.0$, $C = +5.6$) for carbohydrates. [b] Two idealized models for cyclopentanes were used: the underlined values employ ω_{int} values from the cyclopentane electron diffraction data of Adams et al. (1970); the other value, when listed, is based on the molecular mechanic calculated geometries of Hendrickson (1961). [c] We thank G. T. DeTitta for providing internal ring dihedral angles from X-ray structures for the four PGF models employed. [d] No specific correction for the inversion of the C-9 center was employed. In each case a 9β-H was placed at an expectation position based on the ω_{int} values. [e] The measure of fit throughout is $\sum(\Delta J)^2$ where $\Delta J = J_{obsd} - J_{calcd}$. Calculated *J* values were derived from the internal dihedral angles (ω) of the model (or X-ray) cyclopentane structures in the following way: $\phi_{cis} = \omega_{int}$ and $\phi_{trans} = \omega_{int} \pm 124$; the interproton φ values were converted to *J* values by using a modified Karplus equation.[a] For each entry, calculated and observed *J* values for the following vicinal interactions, (8,9), (9,10β), (10β,11), (9,10α), (10α,11), (11,12), and (8,12), were used with equal weighting.

for H-10α at C_s–C9$^\alpha$ and C_2^+–C12. The agreement between the previous independent conformational assignments and predicted chemical shift differences is excellent.

Local Conformational Features in the Side Chains. Two aspects of side-chain conformation have been the focus of attention as possible bases for distinction between $PGF_2\alpha$ and PGE_2 receptors: (1) the disposition of the α-chain near C-9, i.e., $\phi_{8,7}$ and $\phi_{7,6}$ (Langs et al., 1977), and (2) the conformation of the allyl alcohol unit, i.e., $\phi_{12,13}$ and $\phi_{14,15}$ (DeTitta et al., 1980). NOE data bearing on both of these regions was obtained in the present study.

Turning first to the allyl alcohol region, in the vast majority of PG crystal structures the key dihedral angles are found in the following ranges, $\phi_{12,13} = 98$–$128°$ and $\phi_{14,15} = -122 \pm 13°$, which corresponds to the conformational array designated as "normal" Δ^{13} in Figure 1 (see also Figure 8 for the definition of the two dihedrals specified). For $PGF_2\alpha$ a less populated "retro-Δ^{13}" form, $\phi_{12,13} = -122 \pm 9°$ and $\phi_{14,15} = 148°$, has also been observed (DeTitta et al., 1980; DeTitta et al., personal communication). The NOE ratios for H-13 and H-14 upon irradiation at both the C-11β and C-15 methine signals provide a clear distinction between these two conformers. In all analogues examined f_{14}[11β-H] exceeds f_{13}[11β-H] by a significant margin.[6] This suggests that the deviation from the H-12/H-13-anti conformation ($\phi_{12,13} = +120$) is in fact in the rotation sense opposite to that seen in the retro form. For aqueous $PGF_2\alpha$ a $\phi_{12,13}$ value of +80–100° gives an acceptable fit to the NOE data. Methylation at C-16 or C-17 and 1,9-olide closure apparently effect a shift in conformational preference toward $\phi_{12,13} = +120°$. In like manner we conclude that the solution-state value of $\phi_{14,15}$ is in the $-140° \rightarrow -170°$ range with values nearer −120° (=H-15/H-14-anti) increasingly favored in the methylated and 1,9-olide forms. All of the evidence is contrary to the significant population of the retro form in the solution state. The postulated contribution of this form as an explanation for the olefinic region CD couplet must thus be dismissed as most unlikely.

Moving out further toward the ω terminus, the $\phi_{15,16}$ preference is the next question. In solid-state hairpin structures a gauche conformation (typically $\phi_{15,16} = +60$–71) in this site serves to bring the two side chains together. In all prostanoid analogues examined to date, the C-16 methylene is a distinct AB pattern ($\Delta\delta_{16a,b} \approx 0.09$ ppm), and thus, the H-15 multiplet splitting may be assumed to accurately reflect the *J* values. The values observed range from 5.4 to 8.3 Hz, and typically $J_{15,16a}$ and $J_{15,16b}$ differ by 1 Hz or less. Obviously a number of rotamers must be significantly populated to yield these average values. To the extent that a preference can be suggested, the $\phi_{15,16} = -60°$ form provides the best rationale for the coupling data and the significant f_{17}[14] values observed in difference NOE spectra. The $\phi_{15,16} = 180°$ form also appears to contribute significantly.

As to solution-state data bearing on the α-chain conformation, the possible key diagnostics are H-9/H-6, H-9/H-7, H-8/H-6, and H-8/H-7 NOEs and scalar coupling constants in the C-6 → C-8 fragment. Unfortunately, the C-7 methylene appears as an extremely closely coupled ($\Delta\delta_{7a,b} < (1/2)J_{7a,b}$) pattern in the aqueous medium spectra of all analogues reported herein. The H-8 multiplet pattern seen in Figure 5 reveals nonidentical (8,7) splittings, 6.2 and 8.3 Hz, which thus represent a minimum measurement of the differences in the $J_{7,8}$ and $J_{7',8}$ values. During the course of the Pr(III) shift experiment $\Delta\delta_{7a,b}$ increases and the resulting multiplet could be analyzed: the downfield H-7 displayed $^3J = 6.6$ and 7.8 Hz while upfield multiplet splittings were 6.9 and 9.4 Hz. Unfortunately it was not possible to correlate a specific H-7 configuration with the distinct J_8 and J_6 values observed in the two experiments; however, extensive motional averaging of the $\phi_{8,7}$ and $\phi_{7,6}$ can be excluded. In $PGF_2\alpha$ a substantial cross-relaxation occurs between H-9 and H-6 in both D_2O, f_6[9] = 6.8%, and $CDCl_3$, f_6[9] = 5.4%, suggesting an H-6/9β distance about 15% greater then $r_{10\beta,9\beta}$, roughly comparable to the H-8β/9β distance at ca. 0.25 nm. The $PGF_2\alpha$ crystal structures ($\phi_{8,7} = +58°$, $\phi_{7,6} = 140°$ and +128°) correspond to a H-6/9β distance of 0.21–0.23 nm. The observed solution-state scalar and dipolar coupling values can be fitted to general features of the solid-state structures of bis unsaturated PGF_2 derivatives by slight rotations $\phi_{8,7} \rightarrow +30°$ and $\phi_{7,6} \rightarrow +105°$. In contrast, the skeletal dihedral angle values observed for PGE_2 ($\phi_{8,7} = -61°$, $\phi_{7,6} = -127°$), would, if they applied

[6] This is particularly clear in analogues in which the H-13,14 pattern is more nearly first order. In natural $PGF_2\alpha$, $\Delta\nu_{AB} \approx J_{AB}$, and the apparent values of $f_{14}[j]$ and $f_{13}[j]$ observed in any specific saturation difference spectrum have no quantitative validity. In $CDCl_3$ solution, and for other prostanoids, the H-12/H-14 cross-relaxation can be observed: the $\sigma_{12,14}/\sigma_{12,13}$ ratio is greater than 3, indicating a strong H-12/H-14-peri (H-12/H-13-anti) preference [unpublished studies; for one example, see Andersen et al. (1984b)].

to a PGF structure, predict identical $J_{8,7}$ values and essentially no observable 6/9β NOE. The $\phi_{8,7}/\phi_{7,6}$ preferences can thus serve as stereorecognition features for distinguishing PGF and PGE structures at their receptors.

Overall Conformation and Conclusions. Quantitative data bearing on the rotameric preferences in the extreme ends of the side chains (past C-5 and C-16, respectively) are lacking. In crystal structures PGF_2 forms display a variety of $\phi_{5,4}$ values (including +150°, +103°, and −155°). A qualitative analysis of the Pr(III) shift data, with comparison to *n*-alkanoates, indicates similar carboxylate to protons distances for H-2 → H-6, suggesting the lack of a fixed gauche arrangement in the α side chain. The large shift values for both C-7 methylene protons, H-8β, and h-13 indicate that $\phi_{5,4}$ is restricted to values (−60 → −160°) that place the carboxyl terminus nearer the β-face of the cyclopentane ring. This is an unexpected finding and appears to hold for the methylated $PGF_2\alpha$ analogues as well. To the extent that qualitative analysis of Pr(III) shift values based on distance alone (r^{-3} relationship assumed) is valid, the ω-chain terminus must spend most of its time in a region below (α to) the cyclopentane ring in order to generate the small shift values observed for hydrogens at C17 → C20. This serves as an independent confirmation of the negative values of $\phi_{14,15}$ *and* $\phi_{15,16}$ which first arose from analysis of the NOE data. The PG-20 Me/Ln vector is, however, far from being the longest distance in the molecule. In each analogue the ring 10α hydrogen displays the smallest lanthanide-induced shift. Limited studies of Gd(III)-induced changes in relaxation rates (which should display only a distance dependence) confirm that H-10α is the site most remote from the CO_2Ln grouping. The solution conformations of $PGF_2\alpha$ thus bear little resemblance to the "hairpin form" seen in solid-state structures: the side chains are not kept within a common plane. It remains to be determined which of these, if any, are the pertinent models for the receptor-bound state.

A complete picture of the conformational preferences and motional features of $PGF_2\alpha$ did not, however, result from this study. Even at 500 MHz the spectra display regions in which resonances are too crowded for specific NOE experiments. Clearly it will be essential to use transient NOE data, preferably obtained from the buildup of cross-peaks at short mixing times in pure absorption phase NOESY experiments in order to obtain accurate values for the pertinent cross-relaxation rates. The studies detailed herein provide a justification for further use of lanthanide probes since strict specificity for carboxylate binding is now confirmed by the lack of shift (or relaxation) increments for resonances in the immediate neighborhood of the other hydroxyl binding sites. The present study provides the essential preliminaries—resonance assignments, coupling constants, and steady-state NOE values—for this continuing investigation.

Acknowledgments

We thank Cynthia J. Hartzell for sample preparation and D. J.-J. Liu for providing the samples of $PGF_2\alpha$ macrocyclic lactones. We also thank the M. J. Murdock Charitable Trust for support for the departmental NMR facility, Alvin Kwiram and Brian Reid for efforts to secure this support, and Gary Drobny for maintaining the spectrometers and technical advice.

Registry No. $PGF_2\alpha$, 551-11-1; 15-*epi*-$PGF_2\alpha$, 37658-84-7; 16,16-dimethyl-$PGF_2\alpha$, 39746-23-1; 17,17-dimethyl-$PGF_2\alpha$, 80648-19-7; $PGF_2\alpha$-1,9-olide, 55314-48-2; $PGF_2\alpha$-1,15-olide, 55314-49-3; $PGF_2\alpha$ methyl ester, 33854-16-9.

References

Abrahamsson, S. (1963) *Acta Crystallogr. 16*, 409.
Adams, W. J., Geise, H. J., & Bartell, L. S. (1970) *J. Am. Chem. Soc. 92*, 5013.
Andersen, N. H. (1985) in *Handbook of Biology and Chemistry of Prostaglandins and Related Metabolites of Polyunsaturated Fatty Acids* (Curtis-Prior, P. B., Ed.) Churchill–Livingstone, Edinburgh, Scotland (in press).
Andersen, N. H., & Leovey, E. M. K. (1974) *Prostaglandins 6*, 361.
Andersen, N. H., & Ramwell, P. W. (1974) *Arch. Intern. Med. 133*, 30.
Andersen, N. H., Ramwell, P. W., Leovey, E. M. K., & Johnson, M. (1976) *Adv. Prostaglandin Thromboxane Res. 1*, 271.
Andersen, N. H., Imamoto, S., & Picker, D. H. (1977) *Prostaglandins 14*, 61.
Andersen, N. H., Subramanian, N., Imamoto, S., Picker, D. H., Ladner, D. W., McCrae, D. A., Lin, B.-S., & De, B. (1981a) *Prostaglandins 22*, 809.
Andersen, N. H., Imamoto, S., & Subramanian, N. (1981b) *Prostaglandins 22*, 831.
Andersen, N. H., Imamoto, S., Subramanian, N., Picker, D. H., Ladner, D. W., De, B., Eggerman, T. L., Harker, L. A., Tynan, S. S., Robertson, R. P., Oien, H. G., Rao, Ch. V., Lindberg, M., & Naqvi, R. (1981c) *Prostaglandins 22*, 841.
Andersen, N. H., Lin, B.-S., & Nguyen, K. T. (1984a) *Biochem. Biophys. Res. Commun. 121*, 702.
Andersen, N. H., Eaton, H. L., & Nguyen, K. T. (1984b) *Tetrahedron Lett. 25*, 5259.
Anteunis, M., & Danneels, D. (1975) *Org. Magn. Reson. 7*, 345.
Chapman, G. E., Abercrombie, B. D., Cary, P. D., & Bradbury, E. M. (1978) *J. Magn. Reson. 31*, 459.
Conover, W. W., & Fried, J. (1974) *Proc. Natl. Acad. Sci. U.S.A. 71*, 2157.
DeTitta, G. T., Langs, D. A., & Erman, M. G. (1980) *Adv. Prostaglandin Thromboxane Res. 6*, 381.
Durette, P. L., & Horton, D. (1971) *Org. Magn. Reson. 3*, 417.
Elgavish, G. A., & Reuben, J. (1976) *J. Am. Chem. Soc. 98*, 4755.
Hendrickson, J. B. (1961) *J. Am. Chem. Soc. 83*, 4537.
Inagaki, F., & Miyazawa, T. (1981) *Prog. Nucle. Magn. Reson. Spectrosc. 14*, 67.
Kotovych, G., Aarts, G. H. M., Nakashima, T. T., & Bigam, G. (1980a) *Can. J. Chem. 58*, 974.
Kotovych, G., Aarts, G. H. M., & Bigam, G. (1980b) *Can. J. Chem. 58*, 1577.
Kotovych, G., & Aarts, G. H. M. (1982) *Can. J. Chem. 60*, 2617.
Langs, D. A., Erman, M., & DeTitta, G. T. (1977) *Science (Washington, D.C.) 197*, 1003.
Leovey, E. M. K., & Andersen, N. H. (1975a) *J. Am. Chem. Soc. 97*, 4148.
Leovey, E. M. K., & Andersen, N. H. (1975b) *Prostaglandins 10*, 789.
Lin, B.-S. (1983) Ph.D. Thesis, University of Washington.
Murakami, A., & Akahori, Y. (1977) *Chem. Pharm. Bull. 25*, 2870.
Perly, B., & Chachaty, C. (1982) *J. Magn. Reson. 49*, 397.
Rabinowitz, I., Ramwell, P. W., & Davison, P. (1971) *Nature (London), New Biol. 233*, 88.